# Optical transitions and frequency upconversion of $Er^{3+}$ ions in $Na_2O \cdot Ca_3Al_2Ge_3O_{12}$ glasses

**H. Lin, E. Y. B. Pun, and S. Q. Man**

*Department of Electronic Engineering, City University of Hong Kong, Tat Chee Avenue, Kowloon, Hong Kong, China*

**X. R. Liu**

*Changchun Institute of Optics, Fine Mechanics and Physics, Chinese Academy of Sciences, Changchun 130022, China*

Received July 7, 2000

$Er^{3+}$-doped and $Er^{3+}/Yb^{3+}$-codoped $Na_2O \cdot Ca_3Al_2Ge_3O_{12}$ glasses that are suitable for use in optical waveguide devices have been fabricated and characterized. The density, the refractive indices, the optical absorption, the Judd–Ofelt parameters, and the spontaneous transition probabilities of the glasses have been measured and calculated. Intense 1.533-$\mu$m fluorescence was observed in these glass systems under 798- and 973-nm excitation, and the quantum efficiency was ~100%. Efficient upconversion luminescence at 525, 547, and 659 nm at room temperature was also observed. At a pump intensity of 1220 W/cm$^2$ at 798 nm, frequency upconversion efficiencies of $0.98 \times 10^{-2}$ and $1.03 \times 10^{-2}$ were obtained for green and red emissions, respectively. The standardized value for green emission is higher than those reported for lead germanate, lead tellurium germanate, silicate, and phosphate glasses. Under 973-nm excitation, the enhancement of 1533-nm emission and visible upconversion fluorescence in $Er^{3+}/Yb^{3+}$-codoped glasses are confirmed, and the sensitizing is due to efficient energy transfer from $Yb^{3+}$ to $Er^{3+}$. 

*OCIS codes:* 160.5690, 160.3130, 160.2750, 190.7220, 250.5230, 300.6280.

## 1. INTRODUCTION

Rare-earth-doped oxide glasses that possess high chemical durability and thermal stability are excellent materials for optoelectronics applications.[1–4] Of the oxide glasses, germanate glass is one of the most promising hosts for waveguide lasers and amplifiers, frequency upconversion devices, and Bragg grating devices because of its lower phonon energy, high transparency in a wide wavelength range, and high degree of photosensitivity.[5–7] In addition, aluminate glass attracts much attention because its phonon energy is lower than those of borate, phosphate, silicate, and germanate glasses. Inasmuch as the emission quantum efficiency from a given level depends strongly on the phonon energy of the host medium, it can be expected that the nonradiative loss to the lattice will be small and that the fluorescence quantum efficiency will be high in both aluminate and germanate glasses.

For optical communication systems and upconversion luminescence materials, many trivalent rare-earth ions such as $Er^{3+}$, $Tm^{3+}$, and $Pr^{3+}$ have been used as luminescence centers.[8–12] Among these rare-earth ions, $Er^{3+}$ is the most popular as well as one of the most efficient, and $Er^{3+}$-doped waveguide laser and upconversion laser operations have been achieved at room temperature.[3,13] However, because $Er^{3+}$-doped glasses act as three-level gain systems at 1.5 $\mu$m, codoping with $Yb^{3+}$ is often used to enhance the absorption and pumping efficiencies in short-length active materials employed in compact laser devices and high-power optical amplifiers.[14–16] Unlike for fluoride glasses, upconversion is seldom observed in oxide glasses with high phonon energies and can be realized only in oxide glasses with low phonon energies, such as heavy-metal oxides, gallate, aluminate, and germanate glasses, which exhibit efficient upconversion even at room temperature.

Now research is continuing with the goal of optimizing germanate glasses to obtain higher-quality optical and laser glasses. In this paper we report on the fabrication and characterization of $Er^{3+}$-doped and $Er^{3+}/Yb^{3+}$-codoped $Na_2O \cdot Ca_3Al_2Ge_3O_{12}$ glasses. The composition of these glasses is similar to that of calcium aluminum germanate garnet (CAGG) polycrystal, except for the addition of $Na_2O$. Excellent upconversion properties such as three-photon blue upconversion and efficient green and red upconversion of $Er^{3+}$ in CAGG polycrystalline have been reported.[17] Applications, however, are limited because of the polycrystalline's powder form. Compared with polycrystalline, glass has many advantages, such as stability and easy fabrication into optical fibers and waveguides. $Na_2O \cdot Ca_3Al_2Ge_3O_{12}$ glasses can be regarded as improvements of CAGG polycrystalline and can be expected to possess the advantages of both germanate glasses and CAGG polycrystalline. $Na_2O$ was added to make the glasses suitable for the fabrication of optical waveguide devices by ion exchange. In addition, $Na_2O \cdot Ca_3Al_2Ge_3O_{12}$ glasses contain no heavy-metal oxides, which lower the transparency in the UV-wavelength region, and the presence of ~50% $GeO_2$ is attractive because a direct UV writing technique can be used to make waveguide devices.[18,19]

The optical absorption, the luminescence, and the upconversion fluorescence properties of these glasses were

 

investigated. The spontaneous-emission probabilities for various transitions were predicted from Judd-Ofelt theory. Intense infrared fluorescence and efficient green and red upconversion emissions were observed. The fluorescence and upconversion mechanisms and efficiencies are discussed and estimated here.

## 2. EXPERIMENTS

$Er^{3+}$-doped and $Er^{3+}/Yb^{3+}$-codoped $Na_2O \cdot Ca_3Al_2Ge_3O_{12}$ glasses were prepared from calcium carbonate ($CaCO_3$), aluminum oxide ($Al_2O_3$), germanium oxide ($GeO_2$), sodium carbonate ($Na_2CO_3$), erbium oxide ($Er_2O_3$), and ytterbium oxide ($Yb_2O_3$) powders according to the formula $Na_2O(Na_2CO_3)$–$3CaO(CaCO_3)$–$Al_2O_3$–$3GeO_2$ : 1.0 wt. %$Er_2O_3$ (sample 1) and $Na_2O(Na_2CO_3)$–$3CaO(CaCO_3)$–$Al_2O_3$–$3GeO_2$ : 1.0 wt. % $Er_2O_3$, 4.12 wt. %$Yb_2O_3$ (sample 2). All powders (99.5–99.999% purity) were obtained from Strem Chemical Company. First the well-mixed raw materials were heated for several hours in an $Al_2O_3$ crucible (electric furnace) at 1000 °C, and afterward a higher melting temperature, ~1500 °C, was used. The glasses were subsequently annealed at lower temperatures and then sliced and polished to dimensions of 20 mm × 10 mm × 4 mm. The density of the samples was 3.103 g/cm$^3$; thus the number densities of $Er^{3+}$ and $Yb^{3+}$ ions in the glasses were $9.772 \times 10^{19}$/cm$^3$ and $3.909 \times 10^{20}$/cm$^3$, respectively.

The refractive indices of the glasses were measured at two wavelengths. For sample 1, $n = 1.6224$ and $n = 1.6048$ at $\lambda = 632.8$ nm and $\lambda = 1550$ nm, respectively. For sample 2, $n = 1.6259$ and $n = 1.6078$ at $\lambda = 632.8$ nm and $\lambda = 1550$ nm, respectively. The refractive indices of the two samples at other wavelengths can be calculated from Cauchy's equation $n = A + B/\lambda^2$, where $A = 1.6013$, $B = 8457\,\text{nm}^2$ and $A = 1.6042$, $B = 8697\,\text{nm}^2$ for samples 1 and 2, respectively.

Absorption spectra were obtained with a Perkin-Elmer UV/visible/near-IR Lambda 19 double-beam spectrophotometer. Fluorescence spectra of $Er^{3+}$-doped glasses were recorded with a Spex 500M monochromator and detected, depending on the spectral region, by a photomultiplier or a liquid-nitrogen-cooled germanium detector. 798- and 973-nm beams from a Ti:sapphire tunable laser pumped by an argon laser were used as the excitation sources. The fluorescence lifetime for the $^4I_{13/2}$ level of $Er^{3+}$ was measured with a modulated light source and a HP546800B 100-MHz oscilloscope. In the $^4S_{3/2}$ level and $^4F_{9/2}$ level lifetime measurements, a 521-nm laser with a 4-ns pulse width from an optical parametric oscillator (Opotek MagicPrism VIR) pumped by the 355-nm line of a Nd:YAG laser was used as the pump source, and the decay curves were monitored with a HP5452A 500-MHz oscilloscope.

## 3. RESULTS AND DISCUSSION

### A. Absorption Spectrum and Judd–Ofelt Analysis

The absorption spectrum of sample 1 is shown in Fig. 1. The band assignments are also indicated in the figure.

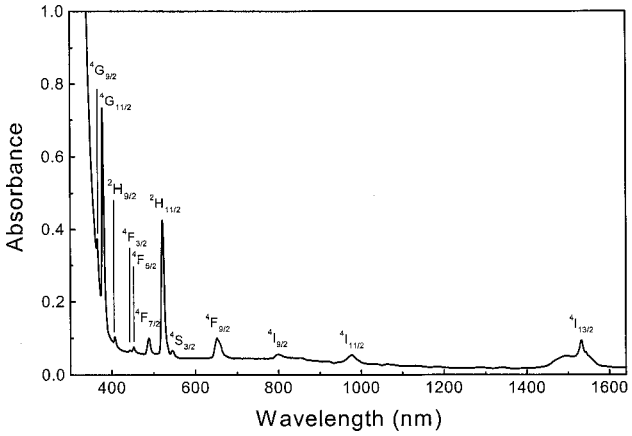


Fig. 1. Absorption spectrum of 1.0-wt. % $Er^{3+}$-doped $Na_2O \cdot Ca_3Al_2Ge_3O_{12}$ glasses.

The radiative transition within the $4f^n$ configuration of a rare-earth ion can be analyzed by the Judd–Ofelt approach. According to the Judd–Ofelt theory,[20,21] the oscillator strength, $P_{\text{calc}}[(S, L)J; (S', L')J']$, of an electric-dipole absorption transition from initial state $|(S, L)J\rangle$ to final state $|(S', L')J'\rangle$ depends on three $\Omega_t$ parameters ($t = 2, 4, 6$) as

$$P_{\text{calc}}[(S, L)J; (S', L')J'] = \frac{8\pi^2 mc}{3h\lambda(2J+1)} \frac{(n^2+2)^2}{9n} \times \sum_{t=2,4,6} \Omega_t |\langle (S, L)J \| U^{(t)} \| (S', L')J' \rangle|^2, \quad (1)$$

where $\lambda$ is the mean wavelength of the transition, $m$ is the mass of the electron, $c$ is the velocity of light, $n$ is the refractive index, $h$ is the Planck constant, $\Omega_t$ are the Judd–Ofelt parameters, and $\langle \|U^{(t)}\| \rangle$ are the double reduce matrix elements of unit tensor operators that are considered to be independent of the host matrix.

We can obtain the experimental oscillator strengths $P_{\text{exp}}$ of the transitions by integrating the absorbance for each band, and the relationship is

$$P_{\text{exp}} = \frac{mc^2}{\pi e^2 N} \int \alpha(\bar{v}) d\bar{v}, \quad (2)$$

$$\alpha(\bar{v}) = \frac{\ln[I_0(\bar{v})/I(\bar{v})]}{d} = 2.303E(\bar{v})/d, \quad (3)$$

where $N$ is the number density of rare-earth ions, $e$ is the charge of the electron, $\bar{v}$ is the wave number, $E(\bar{v})$ is the absorbance, and $d$ is the sample thickness.

Inasmuch as experimental oscillator strength contains electric-dipole and magnetic-dipole contributions, one has to subtract the latter from the experimental oscillator strength to obtain the electric-dipole contribution that can be equated with the calculated oscillator strength. The magnetic-dipole contribution, $P_{\text{md}}$, can be obtained from the refractive index of the glass, and quantity $P'$, and $P_{\text{md}} = nP'$, as reported in Ref. 22.

Judd–Ofelt intensity parameters $\Omega_t$ can be derived from the electric-dipole contributions of the experimental oscillator strengths by a least-squares fitting approach.

**Table 1. Measured and Calculated Oscillator Strengths and Judd–Ofelt Intensity Parameters of $Er^{3+}$ in $Na_2O \cdot Ca_3Al_2Ge_3O_{12}$ Glasses**

| Absorption | Energy ($cm^{-1}$) | $P_{exp}$ ($10^{-6}$) | $P_{calc}$ ($10^{-6}$) | Title |
|---|---|---|---|---|
| $^4I_{15/2} \rightarrow {}^4I_{13/2}$ | 6 527 | 1.067 | 0.611($P_{ed}$) | 0.495($P_{md}$) |
| $^4I_{15/2} \rightarrow {}^4I_{11/2}$ | 10 235 | 0.484 | 0.331 | |
| $^4I_{15/2} \rightarrow {}^4I_{9/2}$ | 12 500 | 0.236 | 0.309 | |
| $^4I_{15/2} \rightarrow {}^4F_{9/2}$ | 15 337 | 1.543 | 1.496 | |
| $^4I_{15/2} \rightarrow {}^4S_{3/2}, {}^2H_{11/2}$ | 19 194 | 8.290 | 8.030 | |
| $^4I_{15/2} \rightarrow {}^4F_{7/2}$ | 20 492 | 1.072 | 1.055 | |
| $^4I_{15/2} \rightarrow {}^4F_{5/2}, {}^4F_{3/2}$ | 22 124 | 0.430 | 0.380 | |
| $^4I_{15/2} \rightarrow ({}^2G, {}^4F, {}^2H)_{9/2}$ | 24 570 | 0.369 | 0.341 | |
| $^4I_{15/2} \rightarrow {}^4G_{11/2}$ | 26 455 | 13.665 | 14.185 | |
| $\Omega_2(10^{-20}\,cm^2)$ | | | | 4.81 |
| $\Omega_4(10^{-20}\,cm^2)$ | | | | 1.41 |
| $\Omega_6(10^{-20}\,cm^2)$ | | | | 0.48 |
| Root mean-square deviation ($\times 10^{-7}$) | | | | 2.497 |

The matrix elements given in Ref. 23 are used in the calculation. The measured and calculated oscillator strengths and the Judd–Ofelt intensity parameters of $Er^{3+}$ in $Na_2O \cdot Ca_3Al_2Ge_3O_{12}$ glasses are presented in Table 1. A measure of the fitting is given by the root-mean-square deviation $\delta_{rms}$ between the measured and the calculated oscillator strengths, and the relationship is

$$\delta_{rms} = \left(\frac{\text{sum of squares of deviations}}{\text{number of transitions} - \text{number of parameters}}\right)^{1/2}. \quad (4)$$

The Judd–Ofelt intensity parameters are important for investigating the local structure and bonding in the vicinity of rare-earth ions. The $\Omega_2$ parameter is indicative of the amount of covalent bonding, and the $\Omega_6$ parameter is related to the rigidity of the host.[24] Table 2 shows a comparison of $\Omega$ parameters in $Na_2O \cdot Ca_3Al_2Ge_3O_{12}$:$Er^{3+}$ glasses and in other glasses discussed in Ref. 2. It can be seen that $\Omega_2$ in $Na_2O \cdot Ca_3Al_2Ge_3O_{12}$ glasses is smaller than those in aluminate and germanate glasses but much larger than that in fluoride glasses. Thus $Na_2O \cdot Ca_3Al_2Ge_3O_{12}$ glasses are less covalent than aluminate and germanate glasses, whereas fluoride glasses are more ionic. In addition, $\Omega_6$ in $Na_2O \cdot Ca_3Al_2Ge_3O_{12}$ glasses is larger than that in germanate glasses but smaller than that in aluminate glasses. Thus the rigidity of $Na_2O \cdot Ca_3Al_2Ge_3O_{12}$ glasses is less than those of aluminate and greater than those of germanate glasses.

Some important radiative properties can be calculated by use of the values of $\Omega_t$. The total spontaneous-transition probability is given by

$$A[(S,L)J;(S',L')J'] = A_{ed} + A_{md} = \frac{64\pi^4}{3h\lambda^3(2J+1)} \times \left[\frac{n(n^2+2)^2}{9} S_{ed} + n^3 S_{md}\right], \quad (5)$$

**Table 2. Intensity Parameters, $\Omega_t$ ($10^{-20}\,cm^2$), of $Er^{3+}$ in Some Glasses**

| Glass | $\Omega_2$ | $\Omega_4$ | $\Omega_6$ |
|---|---|---|---|
| Aluminate[a] | 5.60 | 1.60 | 0.61 |
| Germanate[a] | 5.81 | 0.85 | 0.28 |
| Fluoride[a] | 2.91 | 1.27 | 1.11 |
| $Ca_3Al_2Ge_3O_{12} \cdot Na_2O$ | 4.81 | 1.41 | 0.48 |

[a] Ref. 2.

where $A_{ed}$ and $A_{md}$ are the electric-dipole and the magnetic-dipole contributions, respectively. The electric-dipole and magnetic-dipole line strengths $S_{ed}$ and $S_{md}$ are expressed as

$$S_{ed} = e^2 \sum_{t=2,4,6} \Omega_t |\langle (S,L)J \| U^{(t)} \| (S',L')J' \rangle|^2, \quad (6)$$

$$S_{md} = \frac{e^2}{4m^2c^2} |\langle (S,L)J \| L + 2S \| (S',L')J' \rangle|^2. \quad (7)$$

Here we calculated $A_{md}$ by using the values reported for $LaF_3$ and corrected for the refractive-index difference.[25]

The fluorescence branching ratio of transitions from initial manifold $|(S,L)J\rangle$ to lower levels $|(S',L')J'\rangle$ is given by

$$\beta[(S,L)J;(S',L')J'] = \frac{A[(S,L)J;(S',L')J']}{\sum_{S',L',J'} A[(S,L)J;(S',L')J']}, \quad (8)$$

and the radiative lifetime $\tau_{rad}$ of an emitting state is related to the total spontaneous-emission probability of all transitions from this state by

$$\tau_{rad} = \left\{\sum_{S',L',J'} A[(S,L)J;(S',L')J']\right\}^{-1}. \quad (9)$$

Table 3 shows the spontaneous-transition probabilities, the branching ratios, and the calculated lifetimes of the

optical transitions in $Er^{3+}$-doped $Na_2O \cdot Ca_3Al_2Ge_3O_{12}$ glasses. The branching ratios for the transitions $^4S_{3/2} \rightarrow {}^4I_{15/2}$ and $^4F_{9/2} \rightarrow {}^4I_{15/2}$ are 67% and 91%, respectively. Thus it is possible to obtain efficient green and red emissions in the glasses under suitable excitation conditions.

### B. Fluorescence and Upconversion Properties

The fluorescence spectrum of sample 1 under 798-nm excitation is shown in Fig. 2. The 980-nm and 1.533-$\mu$m emission bands are attributed to the $^4I_{11/2} \rightarrow {}^4I_{15/2}$ and the $^4I_{13/2} \rightarrow {}^4I_{15/2}$ transitions, respectively, and the full width at half-maximum for the 1.533-$\mu$m emission band is ~42 nm. The intensity ratio of the emission at 1.533 $\mu$m to the emission at 980 nm is approximately 38:1, indicating intense $^4I_{13/2} \rightarrow {}^4I_{15/2}$ emission of $Er^{3+}$ in $Na_2O \cdot Ca_3Al_2Ge_3O_{12}$ glasses. The measured lifetime $\tau_{meas}$ of the $^4I_{13/2}$ level determined by exponential fitting is ~9.55 ms and is the same as the calculated radiative lifetime within experimental error; hence the quantum efficiency for 1533-nm fluorescence is ~100%.

The 1533-nm emission bands of samples 1 and 2 under 973-nm excitation are shown in Fig. 3. Significant enhancement for the 1533-nm fluorescence can be observed for the sample containing $Yb^{3+}$ ions. This fact can be understood based on the number of available $Er^{3+}$ luminescence centers. As shown in Fig. 4, for a fixed concentration of $Er^{3+}$ the introduction of $Yb^{3+}$ ions increases the optical absorption of the glasses. The population of $^4I_{11/2}$ and $^4I_{13/2}$ levels is increased because of the energy transfer from $Yb^{3+}$ to $Er^{3+}$; consequently, the probability of radiative emission from the $^4I_{13/2}$ level is also increased.

The emission spectrum in the visible-wavelength range of sample 1 under 798-nm excitation is shown in Fig. 5. The green bands at 547 and 524 nm correspond to the $^4S_{3/2} \rightarrow {}^4I_{15/2}$ and $^2H_{11/2} \rightarrow {}^4I_{15/2}$ optical transitions, respectively. The $^2H_{11/2} \rightarrow {}^4I_{15/2}$ emission was observed when the $^4S_{3/2}$ level was excited because the $^2H_{11/2}$ level is populated from the $^4S_{3/2}$ level by means of a fast thermal equilibrium between the two levels. In addition to the two green bands, a weak red emission at 659 nm was also observed and is associated with the $^4F_{9/2} \rightarrow {}^4I_{15/2}$ transition.

In an upconversion mechanism the upconversion emission intensity $I_{UP}$ is proportional to the $m$th power of the IR excitation intensity $I_{IR}$; i.e.,

$$I_{UP} \propto I_{IR}^{m}, \tag{10}$$

where $m$ is the number of IR photons absorbed per visible photon emitted. A plot of $\log I_{UP}$ versus $\log I_{IR}$ yields a straight line with slope $m$. Figure 6 shows such a plot for the 524-, 547-, and 659-nm emissions, and the values of $m$ obtained were 1.91, 1.86, and 1.83, respectively. This result confirms that two photons contribute to the upconversion of the three visible emission bands.

Upconversion efficiency $\eta$ can be determined by comparison of the upconversion luminescence signal with the directly excited signal intensity[26,27]:

**Table 3. Predicted Spontaneous Radiative Transition Rates and Lifetimes of $Er^{3+}$ in $Na_2O \cdot Ca_3Al_2Ge_3O_{12}$ Glasses**

| Transition | Average Frequency ($cm^{-1}$) | $A_{ed}$ ($s^{-1}$) | $A_{md}$ ($s^{-1}$) | $\beta$ | $\tau_{rod}$ (ms) |
|---|---|---|---|---|---|
| $^4I_{13/2} \rightarrow {}^4I_{15/2}$ | 6 527 | 51.7 | 39.4 | 1 | 11.0 |
| $^4I_{11/2} \rightarrow {}^4I_{15/2}$ | 10 235 | 77.6 | | 0.82 | 10.5 |
| $^4I_{13/2}$ | 3 708 | 8.7 | 8.8 | 0.18 | |
| $^4I_{9/2} \rightarrow {}^4I_{15/2}$ | 12 500 | 111.9 | | 0.85 | 7.59 |
| $^4I_{13/2}$ | 5 973 | 18.6 | | 0.14 | |
| $^4I_{11/2}$ | 2 265 | | 1.3 | 0.01 | |
| $^4F_{9/2} \rightarrow {}^4I_{15/2}$ | 15 337 | 1030 | | 0.91 | 0.882 |
| $^4I_{13/2}$ | 8 810 | 57.7 | | 0.05 | |
| $^4I_{11/2}$ | 5 102 | 33.8 | 6.2 | 0.035 | |
| $^4I_{9/2}$ | 2 837 | 2.9 | 2.7 | 0.005 | |
| $^4S_{3/2} \rightarrow {}^4I_{15/2}$ | 18 382 | 488.2 | | 0.67 | 1.37 |
| $^4I_{13/2}$ | 11 855 | 192.9 | | 0.265 | |
| $^4I_{11/2}$ | 8 147 | 15.9 | | 0.022 | |
| $^4I_{9/2}$ | 5 882 | 31.1 | | 0.043 | |
| $^2H_{11/2} \rightarrow {}^4I_{15/2}$ | 19 194 | 6726 | | – | – |
| $^4F_{7/2} \rightarrow {}^4I_{15/2}$ | 20 492 | 1583 | | – | – |
| $^4F_{5/2} \rightarrow {}^4I_{15/2}$ | 22 124 | 570.0 | | – | – |
| $^4F_{3/2} \rightarrow {}^4I_{15/2}$ | 22 624 | 494.0 | | – | – |
| $^2H_{9/2} \rightarrow {}^4I_{15/2}$ | 24 570 | 848.1 | | 0.32 | 0.378 |
| $^4I_{13/2}$ | 18 043 | 1199 | | 0.45 | |
| $^4I_{11/2}$ | 14 335 | 467.4 | 37.9 | 0.19 | |
| $^4I_{9/2}$ | 12 070 | 21.7 | 1.0 | 0.01 | |
| $^4F_{9/2}$ | 9 233 | 25.5 | 44.4 | 0.03 | |
| $^2H_{11/2}$ | 5 376 | | 1.0 | ~0 | |
| $^4F_{7/2}$ | 4 078 | | 0.8 | ~0 | |

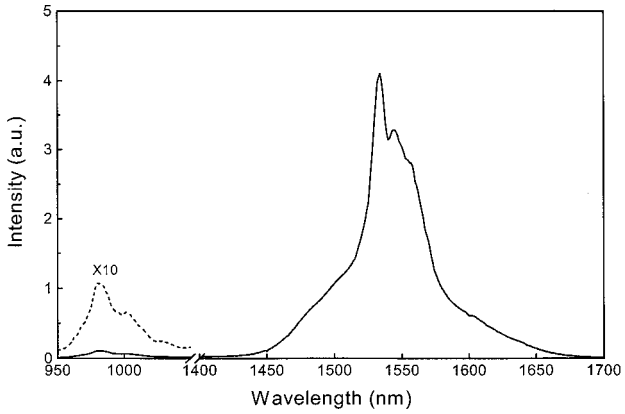


Fig. 2. Fluorescence spectrum of $Er^{3+}$-doped $Na_2O \cdot Ca_3Al_2Ge_3O_{12}$ glasses under 798-nm excitation.

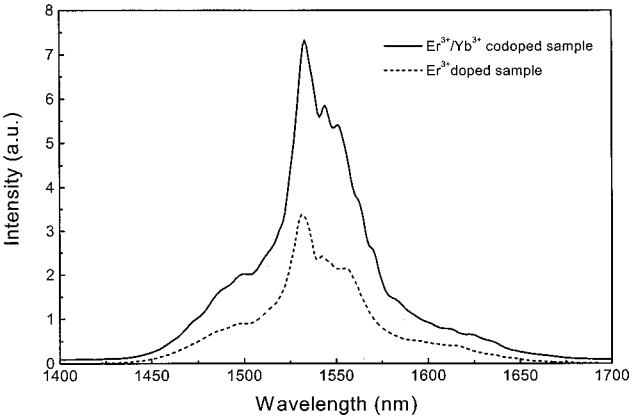


Fig. 3. Fluorescence spectra of $Er^{3+}$-doped and $Er^{3+}/Yb^{3+}$-codoped $Na_2O \cdot Ca_3Al_2Ge_3O_{12}$ glasses under 973-nm excitation.

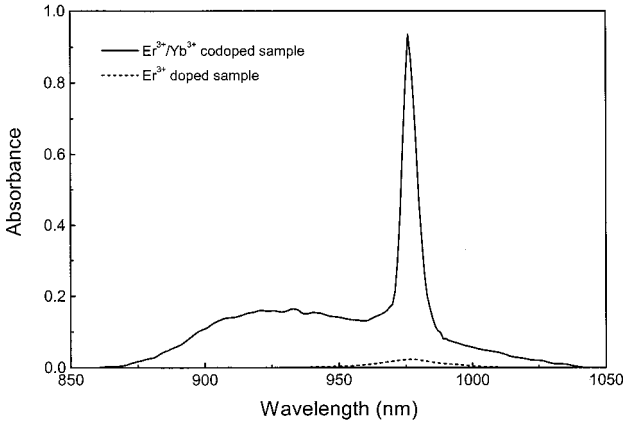


Fig. 4. Absorption spectra of $Er^{3+}$-doped and $Er^{3+}/Yb^{3+}$-codoped glasses near 980 nm.

$$\eta = \eta_q \left[\frac{P_{\mathrm{abs}}(\mathrm{vis})}{P_{\mathrm{abs}}(\mathrm{ir})}\right]\left[\frac{I_{\mathrm{emit}}(\mathrm{upconverted})}{I_{\mathrm{emit}}(\mathrm{direct})}\right]. \tag{11}$$

Here the absorbed light power $P_{\mathrm{abs}}(\mathrm{vis})$ for direct excitation (488-nm pump) and $P_{\mathrm{abs}}(\mathrm{ir})$ for direct excitation (798-nm pump) can be determined from the measured incident light power, the absorption coefficient, and the absorption path length in the sample. The luminescence intensities $I_{\mathrm{emit}}$ (upconverted) and $I_{\mathrm{emit}}$ (direct) are the collected portion of the emitted light at 547 nm measured in the same light-collecting conditions. Quantum efficiency $\eta_q$ for direct excitation is defined as

$$\eta_q = \frac{\tau_{\mathrm{exp}}}{\tau_{\mathrm{rad}}}, \tag{12}$$

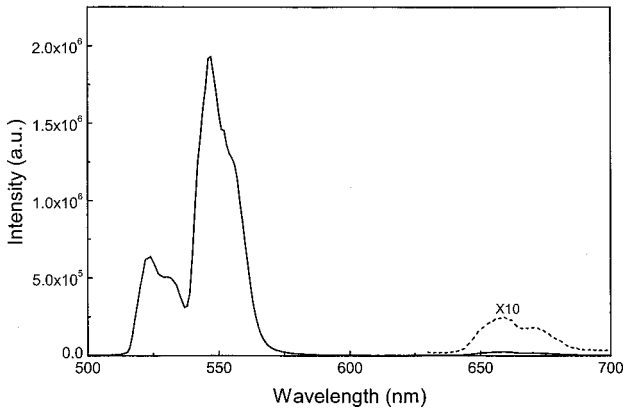


Fig. 5. Upconversion emission spectrum of $Er^{3+}$-doped $Na_2O \cdot Ca_3Al_2Ge_3O_{12}$ glasses under 798-nm excitation.

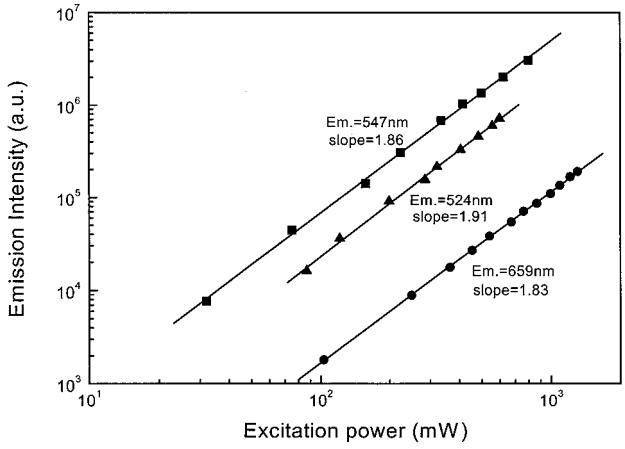


Fig. 6. Dependence of upconversion emission intensity on excitation power under 798-nm excitation for $Er^{3+}$-doped $Na_2O \cdot Ca_3Al_2Ge_3O_{12}$ glasses.

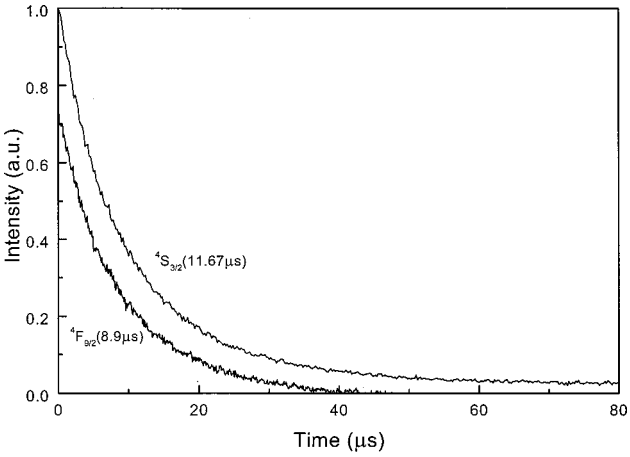


Fig. 7. Fluorescence decay curves for 547- and 659-nm emissions of $Er^{3+}$ in $Na_2O \cdot Ca_3Al_2Ge_3O_{12}$ glasses.

**Table 4. Values of Standardized Green and Red Upconversion Efficiencies of $Er^{3+}$ in Different Types of Glass**

| Glass (Ref.) | $\eta_s$ of Green Upconversion | $\eta_s$ of Red Upconversion |
|---|---|---|
| $Na_2O \cdot Ca_3Al_2Ge_3O_{12}$ | $8.0 \times 10^{-6}$ | $8.4 \times 10^{-6}$ |
| Lead-germanate glass (26) | $3.1 \times 10^{-6}$ | |
| Lead-tellurium-germanate glass (26) | $0.79 \times 10^{-6}$ | |
| Fluoride glass (27) | $1 \times 10^{-3}$ | |
| Silicate glass (27) | $2 \times 10^{-7}$ | |
| Phosphate glasses (27) | $6 \times 10^{-8}$ | |
| Alkali bismuth gallate glasses (28) | $1.3 \times 10^{-3}$ | $3.1 \times 10^{-4}$ |

where $\tau_{exp}$ is the experimentally measured lifetime and $\tau_{rad}$ is the radiative lifetime. From Fig. 7, $\tau_{exp}$ of $^4S_{3/2}$ and $^4F_{9/2}$ in sample 1 were measured to be 11.7 and 8.9 $\mu$s, respectively, and, from the Judd–Ofelt analysis (Table 3), $\tau_{rad}$ were found to be 1.37 ms and 882 $\mu$s, respectively.

When the incident light's power density was 1220 W/cm$^2$, the IR (798 nm) to green (547 nm) and IR to red (659 nm) upconversion efficiencies of sample 1 were determined to be $0.98 \times 10^{-2}$ and $1.03 \times 10^{-2}$, respectively. To compare $\eta$ for various host materials we used a standardized efficiency $\eta_s$ with an incident IR intensity of 1 W/cm$^2$. Because $\eta$ is proportional to the pump power, $\eta_s$ (green at 547 nm) is $8.0 \times 10^{-6}$ and $\eta_s$ (red at 659 nm) is $8.4 \times 10^{-6}$ for $Na_2O \cdot Ca_3Al_2Ge_3O_{12}$:1.0 wt. %$Er_2O_3$ glasses. The standardized upconversion efficiencies of other oxide and fluoride glasses are listed in Table 4. It can be seen that the value of $\eta_s$ (green) is higher than those reported for lead germanate, lead tellurium germanate, silicate, and phosphate glasses but lower than those for fluoride and alkali bismuth gallate glasses.[26–28]

In our experiments, the green and red upconversion fluorescence in sample 1 was easily observed under 798-nm excitation but difficult to see with the naked eye under 973-nm excitation. The possible upconversion mechanisms in the glasses are shown in Fig. 8. When the $^4I_{9/2}$ level is directly excited at 798 nm, the excited energy that is stored in the $^4I_{9/2}$ level relaxes nonradiatively to the $^4I_{11/2}$ and $^4I_{13/2}$ levels. Part of the excitation energy in the $^4I_{11/2}$ level relaxes further, radiatively and nonradiatively, to the $^4I_{13/2}$ level. Under this excitation condition, excited-state absorption (ESA) from the $^4I_{13/2}$ level to the $^2H_{11/2}$ level can occur easily. The energy transfer (ET) through the $^4I_{11/2}$ level and the ESA from the $^4I_{11/2}$ level should also be considered, but their contributions are much smaller than the ESA from the $^4I_{13/2}$ level. However, if the pump source is 973 nm, the ESA from the $^4I_{13/2}$ state cannot occur, because the pump energy is not sufficient to deexcite the excited state of $^4I_{13/2}$ to the $^4S_{3/2}$ state. Hence the green upconversion of sample 1 is rather weak under 973-nm excitation. In addition, for the red upconversion under 798-nm excitation the population of the $^4F_{9/2}$ level is the total result of ET from the $^4I_{13/2}$ level and a contribution from higher-energy levels by nonradiative relaxation. The ET process can be described as $Er^{3+}(^4I_{13/2}) + Er^{3+}(^4I_{11/2}) \rightarrow Er^{3+}(^4F_{9/2}) + Er^{3+}(^4I_{15/2})$, and it is a dominant contribution to red upconversion because the cross relaxation should be efficient as a result of the high population of the $^4I_{13/2}$ level.

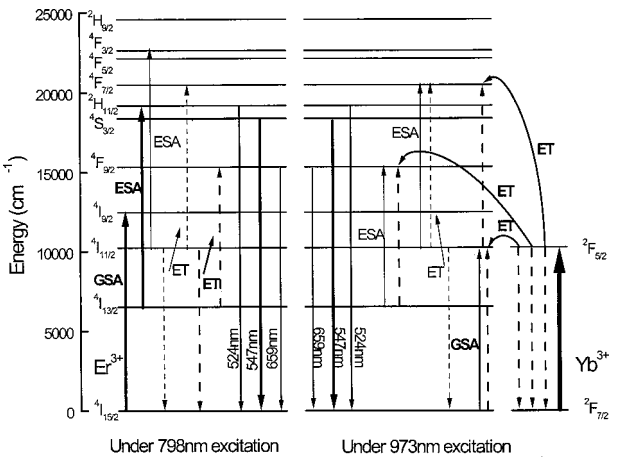


Fig. 8. Energy-level diagram of $Er^{3+}$ and $Yb^{3+}$ in $Na_2O \cdot Ca_3Al_2Ge_3O_{12}$ glasses. Possible upconversion excitation mechanisms under 798- and 973-nm excitation are indicated. The linewidths of the arrows indicate the relative strengths of absorptions and emissions.

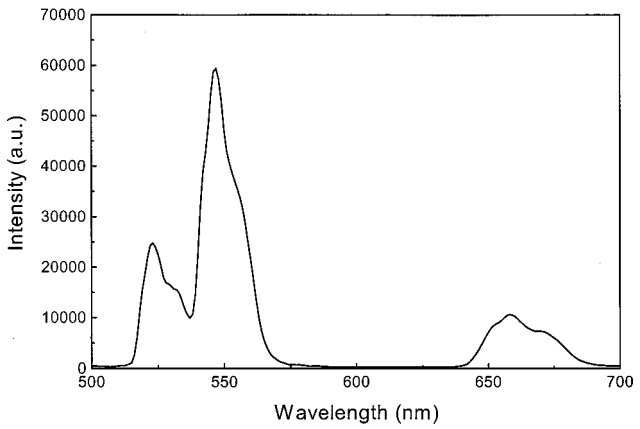


Fig. 9. Upconversion emission spectrum of $Er^{3+}/Yb^{3+}$-codoped $Na_2O \cdot Ca_3Al_2Ge_3O_{12}$ glasses under 973-excitation.

The upconversion of sample 2 is more efficient than that of sample 1 under 973-nm excitation, as shown in Fig. 9, because the doping of $Yb^{3+}$ increases the optical absorption greatly. The plot of $\log I_{UP}$ versus $\log I_{IR}$ for 524-, 525-, and 659-nm emission bands is shown in Fig. 10. From the values of $m$ obtained, the three emission bands also originate from processes that involve two photons. Figure 8 also shows the possible upconversion mechanisms for the green and red bands in sample 2.

The excitation processes for 524- and 547-nm green bands are as follows:

$$Er^{3+}(^4I_{15/2}) + \text{photon} \rightarrow Er^{3+}(^4F_{11/2}), \quad (13a)$$

$$Yb^{3+}(^2F_{7/2}) + \text{photon} \rightarrow Yb^{3+}(^2F_{5/2}), \quad (13b)$$

$$Yb^{3+}(^2F_{5/2}) + Er^{3+}(^4I_{15/2}) \rightarrow Yb^{3+}(^2F_{7/2}) + Er^{3+}(^4I_{11/2}), \quad (13c)$$

$$Yb^{3+}(^2F_{5/2}) + Er^{3+}(^4I_{11/2}) \rightarrow Yb^{3+}(^2F_{7/2}) + Er^{3+}(^4F_{7/2}), \quad (13d)$$

$$Er^{3+}(^4I_{11/2}) + Er^{3+}(^4I_{11/2}) \rightarrow Er^{3+}(^4I_{15/2}) + Er^{3+}(^4F_{7/2}), \quad (13e)$$

$$Er^{3+}(^4I_{11/2}) + \text{photon} \rightarrow Er^{3+}(^4F_{7/2}). \quad (13f)$$

The population of the $^4I_{11/2}$ level increases with $Yb^{3+}$ doping as a result of the efficient energy transfer from $Yb^{3+}(^2F_{5/2})$ to $Er^{3+}(^4I_{11/2})$; hence the probabilities of processes (13e) and (13f) in the $Er^{3+}/Yb^{3+}$-codoped system are higher than those in the $Er^{3+}$ single-doped system. In addition, process (13d) plays an important role in the green upconversion in $Er^{3+}/Yb^{3+}$-codoped systems; thus sample 2 is more efficient than sample 1. Multiphonon relaxation from the $^4S_{3/2}$ level and ESA and ET from the $^4I_{13/2}$ level populate the upper $^4F_{9/2}$ level for the 659-nm red band. Hence the population of the $^4F_{9/2}$ level in codoped glasses is much greater than that in $Er^{3+}$ single-doped glasses; consequently the red upconversion in codoped glasses is also much stronger.

## 4. CONCLUSIONS

$Er^{3+}$-doped and $Er^{3+}/Yb^{3+}$-codoped $Na_2O \cdot Ca_3Al_2Ge_3O_{12}$ glasses have been fabricated and characterized. The $\Omega$ intensity parameters, the radiative rates, the branching ratios, and the fluorescence lifetimes were calculated from Judd–Ofelt theory. Intense fluorescence at 1533 nm and efficient upconversion emissions in $Er^{3+}$-doped and $Er^{3+}/Yb^{3+}$-codoped $Na_2O \cdot Ca_3Al_2Ge_3O_{12}$ glasses were observed at room temperature. In $Er^{3+}$-doped $Na_2O \cdot Ca_3Al_2Ge_3O_{12}$ glasses the quantum efficiency is ~100% for 1533-nm fluorescence, and upconversion efficiencies of $0.98 \times 10^{-2}$ and $1.03 \times 10^{-2}$ were obtained for green and red upconversion emissions, respectively, pumped at 798 nm with a power density of 1220 W/cm$^2$. The value of standardized green upconversion efficiency is higher than those reported for lead germanate, lead tellurium germanate, silicate, and phosphate glasses, and lower than those reported for fluoride and alkali bismuth gallate glasses. Under 973-nm excitation the enhancement of 1.533-$\mu$m emission and visible upconversion fluorescence owing to codoping of $Yb^{3+}$ is confirmed. The upconversion mechanisms of the two glass systems and the sensitization of $Yb^{3+}$ were discussed. From the data obtained, it appears that $Na_2O \cdot Ca_3Al_2Ge_3O_{12}$ glasses are suitable host materials for $Er^{3+}$ and are promising for the fabrication of practical photonic devices because the ion-exchange process and the direct UV writing technique can be used in the glasses for making optical waveguides.

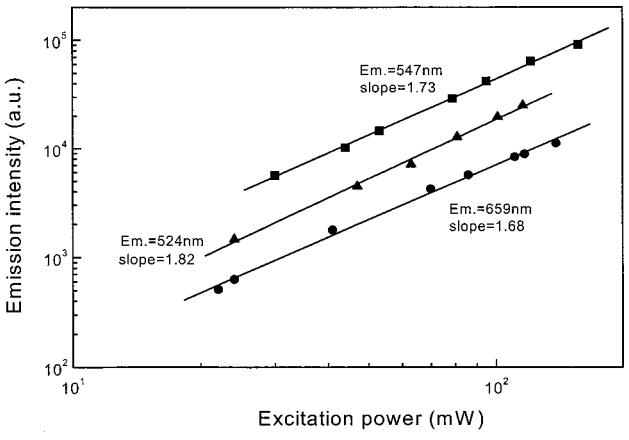


Fig. 10. Dependence of upconversion emission intensity on excitation power under 973-nm excitation for $Er^{3+}/Yb^{3+}$:$Na_2O \cdot Ca_3Al_2Ge_3O_{12}$ glasses.

## ACKNOWLEDGMENT

This research is supported by a Competitive Earmarked Research Grant from the Research Grant Council, Hong Kong.

E. Y. B. Pun's e-mail address is eeeypun@cityu.edu.hk.

## REFERENCES

1. J. E. Roman, P. Camy, M. Hempstead, W. S. Brocklesby, S. Nouth, A. Beguin, C. Lerminiaux, and J. S. Wilkinson, "Ion-exchanged Er/Yb waveguide laser at 1.5 $\mu$m pumped by laser diode," Electron. Lett. **31**, 1345–1346 (1995).
2. X. Zou and T. Izumitani, "Spectroscopic properties and mechanisms of excited state absorption and energy transfer upconversion for $Er^{3+}$-doped glasses," J. Non-Cryst. Solids **162**, 68–80 (1993).
3. G. L. Vossler, C. L. Brooks, and K. A. Winik, "Planar Er: Yb glass ion exchanged waveguide laser," Electron. Lett. **31**, 1162–1163 (1995).
4. K. Hattori, T. Kitagawa, M. Oguma, H. Okazaki, and Y. Ohmori, "Optical amplification in $Er^{3+}$-doped $P_2O_5$-$SiO_2$ planar waveguides," J. Appl. Phys. **80**, 5301–5308 (1996).
5. H. Yamada and K. Kojima, "Upconversion fluorescence in $Er^{3+}$-doped $Na_2O$-$GeO_2$ glasses," J. Non-Cryst. Solids **259**, 57–62 (1999).
6. T. Luo, S. Jiang, G. N. Conti, S. Honkanen, S. B. Mendes, and N. Peyghambarian, "$Ag^+$–$Na^+$ exchanged channel waveguides in germanate glass," Electron. Lett. **34**, 2239–2240 (1998).
7. F. Bucholtz, K. J. Ewing, M. Putnam, and C. G. Askins, "Photoluminescence of Bragg grating in germanosilicate," Electron. Lett. **32**, 1130–1131 (1996).
8. H. Higuchi, M. Takahashi, Y. Kawamoto, K. Kadono, T. Ohtsuki, N. Peyghambarian, and N. Kitamura, "Optical transitions and frequency upconversion emission of $Er^{3+}$ ions in $Ga_2S_3$–$GeS_2$–$La_2S_3$ glasses," J. Appl. Phys. **83**, 19–27 (1998).
9. A. Bjarklev, *Optical Fiber Amplifiers: Design and System Applications*, (Artech House, Boston, Mass., 1993), pp. 1–5.
10. E. Snoeks, G. N. van den Hoven, and A. Polman, "Optimization of an Er-doped silica glass optical waveguide amplifier," IEEE J. Quantum Electron. **32**, 1680–1684 (1996).
11. M. Tsuda, K. Soga, H. Inoue, S. Inoue, and A. Makishima, "Upconversion mechanism in $Er^{3+}$-doped fluorozirconate glasses under 800 nm excitation," J. Appl. Phys. **85**, 29–37 (1999).
12. X. X. Zhang, P. Hong, M. Bass, and B. H. T. Chai, "Blue upconversion with excitation into Tm ions at 780 nm in Yb- and Tm-codoped fluoride crystals," Phys. Rev. B **51**, 9298–9301 (1995).
13. T. J. Whitley, C. A. Millar, R. Wyatt, M. C. Brierley, and D.

Szebesta, "Upconversion pumped green lasing in erbium doped fluorozirconate fibre," Electron. Lett. **27**, 1785–1786 (1991).
14. T. Miyakama and D. L. Dexter, "Cooperative and stepwise excitation of luminescence: trivalent rare-earth ions in $Yb^{3+}$-sensitized crystals," Phys. Rev. B **1**, 70–80 (1970).
15. D. C. Yeh, W. A. Sibley, M. Suscavage, and M. G. Drexhage, "Multiphonon relaxation and infrared-to-visible conversion of $Er^{3+}$ and $Yb^{3+}$ ions in barium-thorium fluoride glass," J. Appl. Phys. **62**, 266–275 (1987).
16. M. P. Hehlen, N. J. Cockroft, T. P. Gosnell and A. J. Bruce, "Spectroscopic properties of $Er^{3+}$- and $Yb^{3+}$-doped soda-lime silicate and aluminosilicate glasses," Phys. Rev. B **56**, 9302–9318 (1997).
17. X. Zhang, J. Yuan, X. Liu, J. P. Jouart, and G. Mary, "Red laser induced upconversion luminescence in Er-doped calcium aluminum germanate garnet," J. Appl. Phys. **82**, 3987–3991 (1997).
18. C. V. Poulsen, J. Hubner, T. Rasmussen, L. U. A. Andersen, and M. Kristensen, "Characterisation of dispersion properties in planar waveguides using UV-induced Bragg grating," Electron. Lett. **31**, 1437–1438 (1995).
19. C. Montero, C. Gomez-Reino, and J. L. Brebner, "Planar Bragg gratings made by excimer laser modification of ion-exchanged waveguide," Opt. Lett. **24**, 1487–1489 (1999).
20. B. R. Judd, "Optical absorption intensities of rare-earth ions," Phys. Rev. **127**, 750–761 (1962).
21. G. S. Ofelt, "Intensities of crystal spectra of rare-earth ions," J. Chem. Phys. **37**, 511–520 (1962).
22. W. T. Carnall, P. R. Fields, and K. Rajnak, "Spectral Intensities of the trivalent lanthanides and actinides in solution. II. $Pm^{3+}$, $Sm^{3+}$, $Eu^{3+}$, $Gd^{3+}$, $Tb^{3+}$, $Dy^{3+}$, and $Ho^{3+}$," J. Chem. Phys. **49**, 4412–4423 (1968).
23. W. T. Carnall, P. R. Fields, and K. Rajnak, "Electronic energy levels in the trivalent lanthanide aquo ions. I. $Pr^{3+}$, $Nd^{3+}$, $Pm^{3+}$, $Sm^{3+}$, $Dy^{3+}$, $Ho^{3+}$, $Er^{3+}$ and $Tm^{3+}$," J. Chem. Phys. **49**, 4424–4442 (1968).
24. C. K. Jorgensen and R. Reisfeld, "Judd–Ofelt parameters and chemical bonding," J. Less-Common Met. **93**, 107–112 (1983).
25. M. J. Weber, "Probabilities for radiative and nonradiative decay of $Er^{3+}$ in $LaF_3$," Phys. Rev. **157**, 262–272 (1967).
26. Z. Pun, S. H. Morgan, K. Dyer, A. Ueda, and H. Liu, "Host-dependent optical transitions of $Er^{3+}$ ions in lead-germanate and lead-tellurium-germanate glasses," J. Appl. Phys. **79**, 8906–8913 (1996).
27. R. S. Quimby, M. G. Drexhage, and M. J. Suscavage, "Efficient frequency up-conversion via energy transfer in fluoride glasses," Electron. Lett. **23**, 32–33 (1987).
28. S. Q. Man, E. Y. B. Pun, and P. S. Chung, "Upconversion luminescence of $Er^{3+}$ in alkali bismuth gallate glasses," Appl. Phys. Lett. **77**, 483–485 (2000).